

AD-A200 060

9

DTIC FILE COPY

ANNUAL TECHNICAL SUMMARY AND STATUS REPORT

Columbia University, Department of Physics,
New York, NY

DTIC
ELECTE
OCT 14 1988
S D

submitted to

Office of Naval Research

Contract N00014-79-C-0769

Period: October 1987 - September 1988

T. C. Marshall

Professor of Applied Physics

DISTRIBUTION STATEMENT A
Approved for public release
Distribution Unlimited

88 1012 065

CONTENTS

I.	Summary	Page 2
II.	Publications and Presentations	5
III.	Status Report	6
IV.	Appendices	7

RE: Distribution Statement
Approved for Public Release. Distribution
Unlimited.
Per Mrs. Catherine M. McKelleget, ONR/Code
1112

Accession For	
NTIS GRA&I	<input checked="" type="checkbox"/>
DTIC TAB	<input type="checkbox"/>
Unannounced	<input type="checkbox"/>
Justification	
By <i>per call</i>	
Distribution	
Availability Codes	
Dist	Availability or Special
<i>A-1</i>	



I. SUMMARY

A. Optical Guiding

We have completed our studies of optical guiding in the exponential gain regime during the past year. These studies show the quality of the guiding is good and behaves as expected using our 2D single frequency waveguide FEL code. Guiding requires a strong pump field and high beam current. The beam filling factor is considerably enhanced by the guiding. These studies were done for optical guiding under conditions where the refractive guiding effects dominate over the gain guiding effects (previous studies by others chiefly explored the gain-guiding limiting case). We have also been studying how optical guiding "performs" along tapered undulators; we find (numerically) that some optical power leaks off the electron beam, and we are going to design undulators to check how guiding is working along the tapered undulator. These studies will form part of the work we propose for the next funding period. The optical guiding studies in the exponential gain regime are discussed in more detail in Appendix I.

B. Sidebands

Experimental results showing that the sideband radiation from a tapered undulator "efficiency-enhanced" FEL oscillator was diminished compared with the sideband power from an untapered FEL have been interpreted using a 2D waveguide code which incorporates three wavelengths (the carrier and two sidebands). The code predicts an appreciable decrease in the long wavelength (strongest) sideband growth rate. A different code, run at NRL for a 10micron FEL, shows similar effects. Thus our conclusions are:

- a) Single wavelength codes are adequate for designing tapered undulator FELs;

b) Tapering reduces sideband power; c) Sidebands will not destroy the principle of FEL efficiency-enhancement.

We have also studied how optical guiding affects the sidebands experimentally and theoretically. As optical guiding modifies the refractive index, it also changes the wave group velocity and therefore changes the location of the sidebands with respect to the carrier wavelength. The spacing between the carrier and the sideband increases as guiding occurs in the end of the zone of exponential growth, and then decreases as guiding is reduced and/or saturation sets in. We have seen these effects experimentally-- adjusting the undulator length to move in or out of saturation, and changing the undulator field to change the optical guiding-- and recently we have been successful in modelling these results using a 1D code. This code lets us predict the sideband location because the refractive terms permit a calculation of the group velocity. A 2D code is now being used to refine this calculation. We also find that our sideband conclusions as stated in the previous paragraph are qualitatively consistent with sideband radiation observed from a tapered undulator where optical guiding is occurring (there was no guiding occurring in our first tapered undulator FEL experiments). Our principal conclusion tentatively is:

- a) Optical guiding has a weak effect on sidebands, mostly their location;
- b) However, sidebands seem to have little effect on guiding-- therefore, codes which calculate optical guiding with no sidebanding are probably reasonably accurate.

These studies thus far are described in Appendix II; the research is continuing.

C. Intra-Cavity Etalon

We have taken spectra of the FEL power when the device uses a single metallic mesh mirror and when a double-mesh, adjustable separation, reflector is used. The linewidth in the former case is much wider than in the latter case. This occurs because the double-mesh

etalon has a wide spacing of longitudinal modes, which will not support an oscillation on the broad band of closely-spaced modes from the long FEL cavity. Thus an intra-cavity etalon will be useful to improve FEL coherence whenever the FEL system gain is large enough to accommodate the additional losses from the etalon.

D. Inverse FEL

We have completed calculations concerning an inverse FEL accelerator which uses a laser in a novel configuration which generates a "diffraction-free" optical beam. This overcomes one of the principal limitations of the conventional inverse FEL accelerator, to wit, the lack of optical guiding of the laser on the electron beam which is being accelerated. However, the price that must be paid for the new technique is higher total energy in the laser pulse. This is not wasted; the energy flows into the electrons over the accelerator path length. Our calculations show that good acceleration gradients and good electron beam quality can be obtained while still trapping a large fraction of the electrons. The "catch" is that the undulator bore must be "large" to accommodate the "large" diameter laser beam.

E. Spiking

High power mode-locked spikes have been observed on certain shots from our FEL. We have begun a theoretical study to identify what mechanisms in the FEL interaction may be responsible for this effect. Mode locking has been reported previously in a brief note from a Japanese FEL, but the mechanism they report, involving a widely dispersed electron energy spectrum, is not convincing.

II. PUBLICATIONS AND PRESENTATIONS

"Observations of Optical Guiding in a Raman Free Electron Laser", A. Bhattacharjee, SY Cai, SP Chang, JW Dodd, TC Marshall, Phys Rev Lett 60, 1254 [1988]

"Efficiency and Sideband Observations of a Raman FEL Oscillator with a Tapered Undulator" FG Yee, TC Marshall, SP Schlesinger, IEEE Trans Plasma Science 16, 162 [1988]

"Diffraction-Free Optical Beams in an Inverse Free Electron Accelerator, SY Cai, A. Bhattacharjee, TC Marshall, Nucl Instruments & Meth in Phys Research, , [1988]

"Generation of Squeezed Radiation from an FEL", I. Gjaja and A Bhattacharjee, Phys Rev A36, 5486 [1987]

"Relativistic Quantum Dynamics and Quantum Noise in Short-Wavelength FELs", I Gjaja and A Bhattacharjee, Phys Rev A37, 1009 [1988]

"Optical Guiding and Sideband Experiments from the Columbia Raman FEL", TC Marshall, AIP Conference Proceedings of the ONR sponsored Non-neutral Plasma Physics Symposium, Washington DC, March 1988.

At the Tenth International FEL Conference, Israel, August-September 1988:

"Sideband Instabilities and Optical Guiding in an FEL"(Invited);

"Effect of Optical Guiding on Sideband Instabilities in a FEL";

"Acceleration of Particles Due to Laser-Plasma Interactions in IFELA"

III. STATUS REPORT

Graduate Students

FG Yee — dissertation completed 9/30/88; tech report

JW Dodd — research in progress(expt); NSF supports him now

SY Cai — research in progress(theor)

SP Chang — research in progress(expt); Taiwan fellowship

I Gjaja — return from Yugo military service; BNL fellow.

T Tanabe — BNL fellow(storage ring FEL)

JS Cao — research in progress (theor.)

Other Support for Principal Investigator:

DEFG082ER53222, "High Beta Tokamak Research" [DOE]

ECS-87-13710, "Optical Guiding in a FEL" [NSF]

Financial-- Current and Projected:

Contract funds, \$160,000 for this project year

Expected Surplus -- None.

Permanent Equipment

Purchased since February, 1988:

2mm waveguide hardware detector, totalling about \$3,000

Observations of Optical Guiding in a Raman Free-Electron Laser

A. Bhattacharjee, S. Y. Cai, S. P. Chang, J. W. Dodd, and T. C. Marshall

Department of Applied Physics, Columbia University, New York, New York 10027

(Received 28 October 1987)

Evidence for optical guiding of 1.7-mm-wavelength radiation along an electron beam in a Raman free-electron laser is obtained experimentally and compared with numerical simulations. Optical guiding is manifest as the interference effect of several waveguide modes; this is observed beyond the point of electron-beam termination. The experiment operates in the regime of exponential signal gain and appreciable electron-beam space charge.

PACS numbers: 42.55.Tb

In the free-electron laser (FEL) the electron beam not only is the source of energy for the growing electromagnetic (EM) field, but can, in addition, distort the wave front and alter the phase velocity of the radiation; this leads to a focusing effect known as optical guiding, which offsets the diffractive spreading of the optical beam. Optical guiding has been studied theoretically in the FEL Compton regime¹⁻⁵ and has been shown to yield guiding over many Rayleigh ranges.

Recently, we have presented calculations⁶ that indicate optical guiding should occur in the Raman regime (conditions of appreciable electron-beam space charge, "weak" undulator field, and "long" wavelength⁷). These calculations account for the presence of an overmoded waveguide, customarily used in order to contain the EM radiation as well as to provide a stable equilibrium geometry for the electron beam. However, the waveguide is not necessary for the containment of the EM fields when optical guiding occurs. Recent experiments⁸ at MIT have found that the mechanisms promoting optical guiding do indeed occur. However, because only the dominant waveguide mode propagates in the MIT FEL, the FEL mechanisms which support optical guiding do not sustain a truly guided wave but rather modify the profile of the radiation intensity near the electron beam⁹; in addition, there are subtleties introduced into their experiment because the electrostatic waves are important.¹⁰ The FEL experiment at Los Alamos National Laboratory has revealed¹¹ a "bending" effect of the radiation contained in the optical resonator. La Sala, Deacon, and Madey have also recently reported on optical guiding influenced by gain guiding effects.¹²

In this Letter we report experimental results, compared in detail with numerical computations, which are consistent with refractive optical guiding effects as they occur in a Raman FEL experiment at Columbia University. In contrast to the MIT experiment, the shorter wavelength in our apparatus permits the excitation of several waveguide TE modes which interfere and permit a truly optically guided beam to form. The interference pattern, which is observed in both the numerical simulations and the experiment, is evidence of optical guiding.

The numerical study, with the 2D FEL and self-consistent electromagnetic equations appropriate for modeling of our system,⁶ describes an electron-beam filament ($r_b = 2$ mm) on the axis of an overmoded cylindrical waveguide ($R = 9$ mm). Other parameters are electron-beam energy 800 kV, current density 2000 A/cm², normalized undulator vector potential $a_w = eB_{\perp} / k_0 mc^2 > 0.3$, helical undulator period $2\pi/k_0 = 17$ mm, and FEL radiation wavelength 1.7 mm. The theory includes the effects of space charge, appropriate to the Raman FEL. The FEL device is operated as a self-amplifier of noise, which grows exponentially to a point of near saturation at the end of the undulator (50 cm) where the optical-guiding effect is observed.

The computations use the Hamiltonian equations for electron dynamics and Maxwell's equation for the normalized vector potential of the radiation field a_r , driven by the transverse source currents which excite the TE modes of the waveguide. These equations are described in detail in Ref. 6. Note that the FEL mode couples to the waveguide via the dispersion relation which predicts the excitation of only a few waveguide modes; however, additional modes can be excited by mode coupling caused by the nonlinearities in the single-particle equations. The higher-order modes are excited at the FEL frequency, but their axial wave numbers differ because of the waveguide dispersion. In Fig. 1(a) is shown an example of optical guiding in a waveguide where ten higher-order modes are excited: Note that the field amplitude grows more rapidly on axis than off axis. Guiding enhances the power gain and growth rate, because the "filling factor" is enhanced. We find that the inclusion of "evanescent" waveguide modes in the calculation results in no change in these results. For computations we assume that the source field at the undulator entry ($z = 0$) is a TE₁₁ mode. Although the values of the field amplitude in Fig. 1(a) are consistent with the experimental situation, we remark that as long as the experiment is operated in the exponential gain regime, the field profile at $z = 50$ cm and the guiding achieved there are not sensitive to the choice of $a_r(0)$, because the system is several e -folding lengths long.

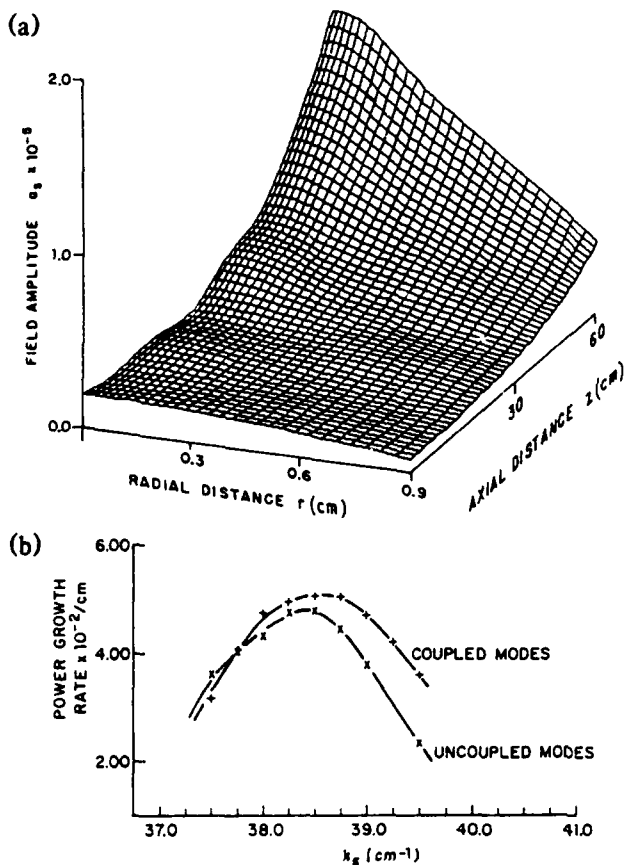


FIG. 1. (a) The exponential growth of 1.7-mm-wavelength optically guided waves on an electron beam in a cylindrical waveguide (drift tube) described in the text. The ordinate is the normalized magnetic vector potential of the FEL radiation and the axial distance is measured along the axis of the beam and undulator. (b) The growth-rate spectrum of the Raman FEL, showing the computed guiding case ("coupled modes") and the unguided case ("uncoupled modes"). The parameters are the same as in the paper, except that the electron-beam radius is 3 mm and the waveguide radius is 12 mm; this accounts for the difference in wavelength. "Antiguinding" occurs for $k < 37.8 \text{ cm}^{-1}$.

In Fig. 1(b) is shown the effect of optical guiding on the growth rate, for slightly different parameters than Fig. 1(a). The guiding can be "turned off" by our calcu-

lating the interaction of the electrons with each TE mode independently and then superimposing the solutions. Note that guiding has less effect on growth for wave numbers less than that of the gain maximum (this asymmetry is a consequence of the space charge). This effect at longer wavelengths can be described as "antiguinding": What happens in this range of wavelengths is that the phase behaves as $d\phi/dz < 0$ rather than $d\phi/dz > 0$. The effect on the wave profile is that of flattening rather than a peaking, and this contributes to a reduction of filling factor and a slight reduction of growth rate. In the experimental study which follows, the FEL is operated in the mode of amplifier of noise, and therefore the signal observed at the end of the undulator has the wavelength corresponding to maximum gain (for which guiding occurs).

The experimental apparatus is shown in Fig. 2. The diode, generation of the electron beam, and apparatus have been already described in detail elsewhere.¹³ The electron beam is abruptly terminated by a polyethylene "witness plate," which permits the 1.7-mm radiation to pass. The intensity profile within the drift tube is examined with use of a "waveguide probe," which consists of a 2-mm-diam cylindrical waveguide fitted with a plastic horn antenna.¹⁴ The local fields in the drift tube launch a guided wave on the dielectric material of the horn, which conveys the radiation into the small waveguide and thence to a Schottky-barrier detector following a high-pass ($\lambda < 2 \text{ mm}$) filter. The characteristic far-field pattern of the probe is a narrow forward-directed lobe having a 3-dB half width $\geq 10^\circ$, with side lobes down by $\approx 15 \text{ dB}$. Prior to measurements of the guiding, the spectrum of the FEL radiation was examined to establish that the correct wavelength was being generated and detected. Also, it was verified that the FEL radiation was growing exponentially along the undulator up to the point of electron-beam termination. The waveguide probe has no effect on the electron-beam equilibrium, and the FEL radiation passes beyond it and diffracts out the open end of the drift tube. The witness plate, 6 mm thick, must be replaced roughly every six shots; this requires a sturdy mechanical jig for the probe so that it can return to its initial position. The experiment uses a

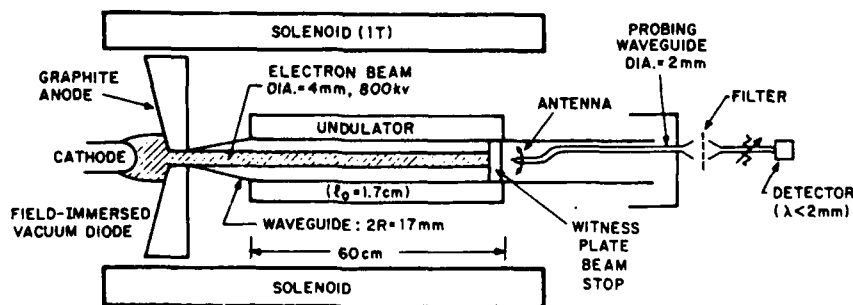


FIG. 2. Schematic of the FEL apparatus. The diode, containing a cold cathode, is attached to a pulse-line accelerator. The waveguide probe diagnostic is located behind the "witness plate," which is at the end of a 50-cm-long undulator.

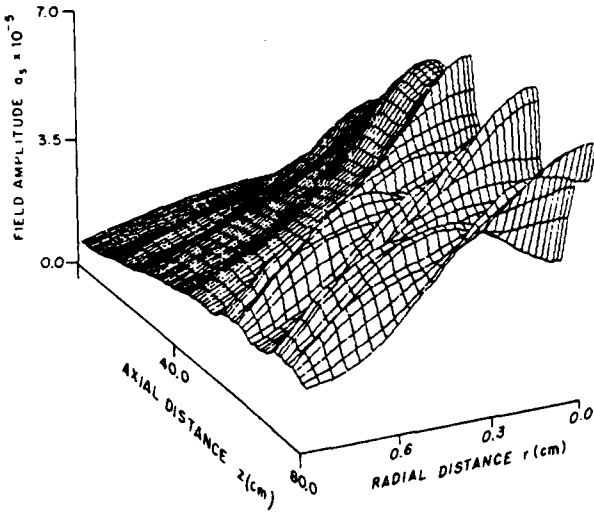


FIG. 3. A view of the computed optically guided radiation shown in Fig. 1(a) when the electron beam is terminated at $z=50$ cm and the EM waves proceed down the empty waveguide. If the modes are decoupled, the intensity would be nearly constant beyond the termination point.

constant magnetic field (≈ 1 T) for electron-beam guiding and focusing. As the FEL frequency is far above the electron gyrofrequency, the only physical effect of the guiding field is to enhance the electron quiver motion in the undulator. We model the guiding-field effect in the theory with use of an undulator magnetic vector potential which will produce the level of quiver motion obtained in the experiment.

In Fig. 3 is shown a computation for the radiation

propagating beyond the witness-plate termination [same conditions as Fig. 1(a)]. One should note a characteristic "sloshing" of the radiation in the waveguide, resulting in periodic maxima along the z axis and off-axis local minima correlating with minima on axis. This is caused by the interference of the several modes responsible for the optical guiding; these modes, having different radial and axial wave numbers, account for the complex radiation pattern beyond the witness plate. (If the modes are artificially decoupled, in which event there can be no guiding, the radiation is dominated by the TE_{11} mode and no such interference pattern results.) The periodicity along the axis depends on the waveguide modes; that is, it is determined by the waveguide size and the operating frequency. The location of the first and subsequent minima does, however, depend on whether there is guiding or "antiguinding"; our calculations show that in the latter case, the positions of the maxima and minima fall on the respective minima and maxima of Fig. 3.

The data are assembled from > 100 shots, selected for nearly identical diode voltage, and are presented in Figs. 4(a)-4(c). The intensity variation along the z axis agrees satisfactorily with the guiding (at gain-maximum) theory. However, if the undulator field is reduced by $\frac{2}{3}$, no such periodicity of intensity along the axis is observed, in agreement with the numerical simulation which predicts virtually no guiding under these conditions. The radial profiles of the intensity at the axial intensity minimum [Fig. 4(b)] and maximum [Fig. 4(c)] also show the expected qualitative features. In Fig. 4(c) is also plotted the TE_{11} intensity distribution for comparison with the prediction of the optical-guiding intensity profile; in this case the intercepts of the theory curves are

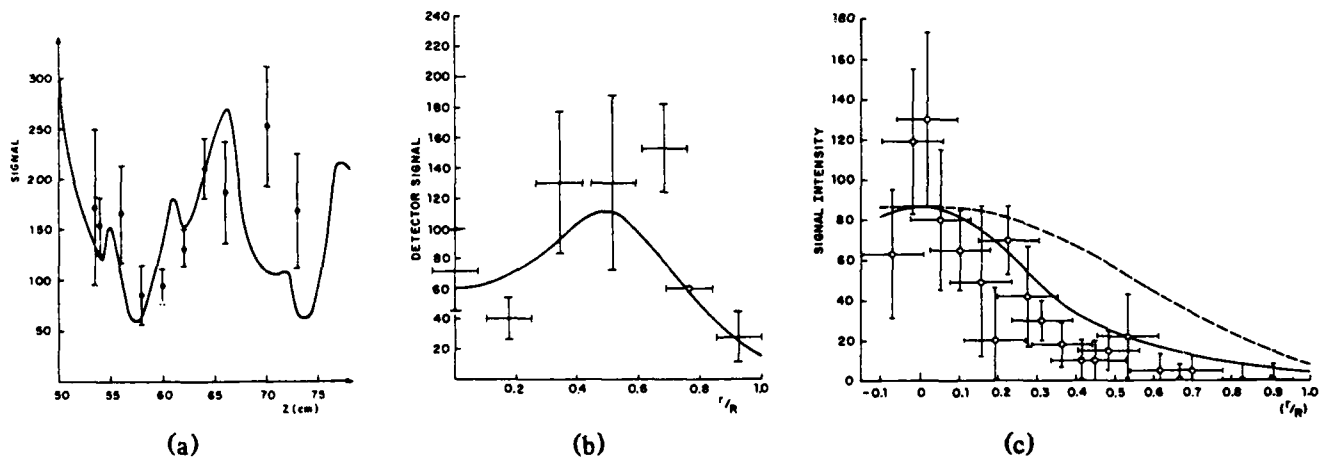


FIG. 4. Experimental data (points) compared with theory (solid or dashed lines) from Fig. 3; the experimental data are the detector signal in millivolts, while the theory scale is arbitrary intensity units. (a) Dependence of intensity along the z axis behind the termination point ($z=50$ cm) of the electron beam. The axial location of the data points is inexact to the extent ≈ 1 cm because of the finite length of the waveguide probe. (b) Radial dependence of intensity at $z=58$ cm and (c) $z=65$ cm. The dashed line in (c) is a plot of the TE_{11} mode intensity which is expected if no optical guiding occurred, and both theory curves are normalized to the same point to fall within the range of the data at $r=0$. The radial resolution of the probe is ≈ 1 mm.

both normalized to the data at $r=0$.

The results shown in Fig. 4 only establish that the intensity is peaked at the point of beam termination, $z=50$ cm, in accord with theoretical prediction. We have also repeated the axial intensity measurements with the beam stop at $z=42$ cm; it was found that the data essentially reproduce Fig. 4(a). This establishes that the intensity maximum has remained centered on the electron beam in the interaction region, which is consistent with the result obtained from the optical guiding simulation [e.g., Fig. 1(a)].

This research was supported by the U.S. Office of Naval Research, Grant No. N0014-79C-0769, and the National Science Foundation, Grant No. ECS-87-13710. The authors appreciate helpful discussions with Professor S. P. Schlesinger regarding the waveguide probe and the cooperation of the Princeton Plasma Physics Laboratory in calibrating it.

¹W. M. Kroll, P. L. Morton, and M. N. Rosenbluth, *IEEE J. Quantum Electron.* **17**, 1436 (1981).

²C.-M. Tang and P. Sprangle, in *Physics of Quantum Elec-*

tronics: Free Electron Generators of Coherent Radiation, edited by S. F. Jacobs and M. Sargent (Addison-Wesley, Reading, MA, 1982), Vol. 9, p. 627.

³G. T. Moore, *Opt. Commun.* **52**, 46 (1984).

⁴E. T. Scharlemann, A. M. Sessler, and J. M. Wurtele, *Phys. Rev. Lett.* **54**, 1925 (1985).

⁵P. Sprangle, A. Ting, and C.-M. Tang, *Phys. Rev. Lett.* **59**, 202 (1987).

⁶S. Y. Cai, A. Bhattacharjee, and T. C. Marshall, *IEEE J. Quantum Electron.* **23**, 1651 (1987).

⁷P. Sprangle, R. A. Smith, and V. L. Granatstein, *Infrared Millimeter Waves* **1**, 274 (1979).

⁸J. Fajans, J. S. Wurtele, G. Bekefi, D. S. Knowles, and K. Xu, *Phys. Rev. Lett.* **57**, 579 (1986).

⁹F. Hartemann, K. Xu, G. Bekefi, J. S. Wurtele, and J. Fajans, *Phys. Rev. Lett.* **59**, 1177 (1987).

¹⁰J. S. Wurtele and J. Fajans, unpublished.

¹¹R. W. Warren and B. D. McVey, *Nucl. Instrum. Methods Phys. Res., Sect. A* **259**, 154 (1987).

¹²J. E. LaSala, D. A. G. Deacon, and J. M. J. Madey, *Phys. Rev. Lett.* **59**, 2047 (1987).

¹³S. C. Chen and T. C. Marshall, *IEEE J. Quantum Electron.* **21**, 924 (1985).

¹⁴M. A. Heald and C. W. Wharton, *Plasma Diagnostics with Microwaves* (Wiley, New York, 1965), p. 334.

Appendix II

Invited Paper to be presented at the Tenth International Free Electron Laser Conference, Jerusalem, Israel, August 29 - September 2, 1988

(to be published, J. Nucl. Instr. & Meth. in Phys. Res.)

SIDEBAND INSTABILITIES AND OPTICAL GUIDING IN A FREE-ELECTRON LASER : EXPERIMENT AND THEORY

A. Bhattacharjee, S.Y. Cai, S. P. Chang, J. W. Dodd, and T. C. Marshall

Department of Applied Physics
Columbia University
New York, New York 10027

Abstract

Experimental and theoretical studies of the effects of tapering and optical guiding on sideband instabilities are reported. The experiments are performed in the Columbia Raman FEL ($\approx 2\text{mm}$). Experiment shows sizeable reductions in sideband amplitudes in an efficiency-enhanced undulator. In the presence of optical guiding in a constant-period undulator, the sideband shift is larger compared with the case when optical guiding does not occur.

The sideband instability [1] in a free-electron laser, driven by the synchrotron motion of the electrons trapped in the ponderomotive potential well, has been regarded as a hazard to FEL efficiency-enhancement schemes such as the variable parameter undulator [2]. The hazard is that uncontrolled growth of the sideband may detrap electrons from the ponderomotive bucket and undermine the efficiency of energy extraction. Strong sidebands have indeed been observed in experiments [3-5].

One of the purposes of the present paper is to describe recent experimental results from the Columbia FEL ($\approx 2\text{mm}$) with a tapered undulator which shows that the sideband amplitude is much lower than with a comparable constant-parameter undulator [6]. Both experiment and numerical simulation indicate that this reduction in sideband amplitude can be accomplished without compromising the standard prescription for efficiency enhancement.

Another purpose of this paper is to report preliminary experimental and theoretical results on the effects of optical guiding on sidebands. The concept of optical guiding has been validated in several experiments [7-10]. Since optical guiding occurs due to modifications in the refractive index of the electron beam which in turn determines the group velocity of the radiation, it is natural to expect that optical guiding should control the slippage between the electron and optical pulses, and hence, the sideband shift.

We begin with a discussion of sideband instabilities in a tapered wiggler. The operating parameters of the Columbia Raman FEL are given in Table 1, and the experimental configuration is shown in Fig. 1. The experiment demonstrated enhancement in efficiency from 4% ("untapered") to 12% ("tapered") — details are given in Ref.[6]. In Fig. 2 we compare the spectra of the radiated power for the untapered and tapered undulators. Fig.2(a) is the spectrum showing the carrier (2.5mm) and u.e long-wavelength sideband (2.6mm) in an untapered undulator. Figure 2(b) shows the corresponding spectrum for a tapered undulator — the sideband amplitude is down by 50% compared with that in the constant-period undulator. Figure 3 shows the power growth along the tapered

section of the undulator ($l_w = 1.45\text{cm}$ for $z \leq 40\text{cm}$). A 1-D simulation predicts an increase of power by approximately a factor of two [11]. The observations indicate that the enhancement in the efficiency of a tapered undulator is approximately in accordance with the prediction of 1-D, single-mode theory. Furthermore, tapering has the salutary effect of reducing the sideband amplitude. In these experiments, optical guiding does not occur. Numerical simulations of the Columbia FEL using a 2-D code with waveguide boundary conditions reproduce qualitative features of the sideband behavior [6]. (Similar numerical results for a short wavelength FEL have also been reported recently by Hafizi et al. [12].)

We now describe the effect of optical guiding on sidebands. The equations of motion for the electrons are,

$$\frac{d\gamma_j}{dz} = -\frac{k_s a_w a_s}{\gamma_j} \sin\psi_j + \frac{2\omega_p^2}{\omega_{sc}} [\langle \cos\psi \rangle \sin\psi_j - \langle \sin\psi \rangle \cos\psi_j] , \quad (1)$$

$$\frac{d\psi_j}{dz} = k_w + k_s - k_s \sqrt{1 - (1 + a_w^2 - 2a_w a_s \cos\psi_j)/\gamma_j^2} + \frac{\partial\phi}{\partial z} , \quad (2)$$

where $\gamma_j mc^2$ is the energy of the j th electron of rest mass m ; ψ_j is the phase of the j th electron with respect to the signal of frequency $\omega_s = k_s c$ and wave number k_s ; $k_w = 2\pi/l_w$ is the wave number of the wiggler; a_w and a_s are respectively the normalized vector potentials of the helical wiggler and signal; $\omega_p^2 = 4\pi n e^2/m$ is the plasma frequency of the electron beam, and ϕ is the phase shift of the radiation field. The second term on the right-hand side of equation (1) describes the effect of space charge.

The 1-D wave equation for the radiation amplitude, assuming it is slowly varying, is

$$\left(\frac{\partial}{\partial z} + \frac{1}{c} \frac{\partial}{\partial t} \right) u(z,t) = \frac{i\omega_p^2 a_w}{k_s c^2} \left\langle \frac{\exp[-i(\psi-\phi)]}{\gamma} \right\rangle , \quad (3)$$

where $u = a_s \exp(i\phi)$. The calculation can be simplified by integrating along the characteristics of equation (3), which motivates the following variable transformations [13]:

$$x = \frac{c}{L_w(c/v - 1)} (t - z/c), \quad y = \frac{c}{L_w(c/v - 1)} (z/v - t). \quad (4)$$

Here L_w is the length of the wiggler. Then equations (1) - (3) transform to

$$\frac{\partial \gamma_j}{\partial x} = -\frac{L_w k_s a_s a_w}{\gamma_j} \sin \psi_j + \frac{2L_w \omega_p^2}{\omega_s c^2} [\langle \cos \psi \rangle \sin \psi_j - \langle \sin \psi \rangle \cos \psi_j], \quad (5)$$

$$\frac{\partial \psi_j}{\partial x} = L_w (k_w + k_s - k_s / \sqrt{1 - (1 + a_w^2 - 2a_w a_s \cos \psi_j) / \gamma_j^2}) + \frac{\partial \phi}{\partial x}, \quad (6)$$

$$\frac{\partial u}{\partial y} = \frac{iL_w \omega_p^2 a_w}{k_s c^2} \left\langle \frac{\exp(-i(\psi - \phi))}{\gamma} \right\rangle. \quad (7)$$

We impose a periodic boundary condition in time. The period is taken to be $\tau = 2\pi/\Delta\omega$, where $\Delta\omega \equiv \omega_r - \omega_s$ and ω_r is the sideband frequency. Equations (5) - (7) are then solved in the cross-hatched domain indicated in Fig.4.

Refractive optical guiding, which occurs because the refractive index n obeys the condition $\text{Re}(n) > 1$, is of primary interest in this paper. Refractive guiding can be artificially reduced to zero in free space by replacing $\langle \exp(-i\psi) / \gamma \rangle$ with $-i \langle \sin \psi / \gamma \rangle$. In what follows, we compare the results of the 1-D simulation with and without optical guiding, and study the effects of space charge. The numerical results are compared with the well-known formula [5],

$$\frac{\Delta\omega}{\omega_s} = \frac{1 - v_w/c}{1 - v_g/c} \frac{N_{\text{synch}}}{N}, \quad (8)$$

where v_g is the group velocity of the radiation and N_{synch} is the number of periods of the synchrotron oscillations within an undulator which has N periods.

The experiment is done in a highly overmoded waveguide, where optical guiding is set up by the nonlinear coupling of higher order propagating waveguide modes via the FEL interaction [10]. Before we present experimental results, we discuss results from

numerical simulations. In Fig. 5, we compare the sideband shift for the parameters listed in Table 1 (appropriate to the larger drift tube) with and without optical guiding, and zero space charge. The effect of guiding clearly enhances the sideband shift, but also increases the sideband amplitude. It is interesting to note that in this case the lower and upper sidebands are exactly symmetric about the carrier when guiding is turned off.

A preliminary calculation by Johnston et al.[15] in the linear regime predicts $v_g/c = 0.936$ for the parameters of Fig. 5. Our numerical results without space charge in this regime is $v_g/c = 0.943$, which is in reasonable agreement with his theory. If the effect of space charge is included, we obtain $v_g/c = 0.959$ in the linear regime. In the saturation regime, we get $v_g/c = 0.955$ without space charge, and $v_g/c = 0.961$ with space charge. Formula (8) then clearly indicates that the sideband shift enhancement due to guiding is generally degraded by the effects of space charge and at saturation.

We now present sideband spectroscopy studies of the Columbia Raman FEL. The spectrum is obtained by a grating spectrometer with a resolving power ~ 100 . Data is accumulated on a shot-by-shot basis, and then is averaged after discarding shots when the accelerator performance is not within tolerance. The FEL is configured as an oscillator, the output mirror generally being a quartz etalon. This etalon has a widely-spaced distribution of longitudinal modes, unlike the FEL resonator where the cavity modes are closely-spaced. The etalon mirror therefore favors oscillation on just one longitudinal mode of the combined system, and this results in improved coherence. The idea is to choose the etalon spacing so that just one longitudinal mode of the etalon falls within the unstable gain-spectrum of the FEL.

A demonstration of the narrowing of the FEL "carrier" is shown in Fig. 6. In Fig. 6(b), the output mirror is a simple wire mesh, whereas in Fig 6(a) the output mirror is an etalon made up of two wire meshes separated by 15mm spacing. The spectral width of the carrier in Fig. 6(a) is $\sim 1.5\%$, whereas in Fig. 6(b) the carrier is much wider — at least 3% or more. A complicating feature is the sideband; the long wavelength sideband in Fig 6(a)

is prominent. We will return to this shortly. In addition to the linewidth narrowing, the etalon can also "pull" the carrier wavelength of the FEL if the etalon spacing is appreciably changed. We have been able to change the carrier wavelength by $\sim 5\%$ using this technique.

In the sideband studies which follow, not only the magnetic field of the undulator, but also the length of the electron beam in the undulator can be changed. This can be done by using a movable piece of iron inside the guiding-field solenoid; the electron beam is deflected to the wall of the drift tube by the iron. The FEL will oscillate over a wide range of electron beam-length, the "start-time" of the oscillator increasing as the beam length is shortened. It is quite possible to operate the system so that, starting from noise, at a high value of undulator field the signal saturates before reaching the end of the undulator. The sideband can be observed either when the FEL signal reaches a saturated condition (which is where one might naturally expect to find it), or relatively "late" in the regime of exponential growth. This occurs in this experiment because the growth rate of the sideband is comparable to the carrier. When we report data on the sideband in the linear regime of growth, we have shortened the beam length so that saturation does not occur on a single pass, and we observe the signal strength on the first pass of the radiation along the system. The experimental studies use the FEL as an oscillator with a quartz etalon mirror, and couple the output power into the spectrometer where both the carrier and sidebands are observed. (In previous optical guiding studies [10], a broadband filter was used so that the guiding signal data included carrier and sidebands).

Three sideband spectra are shown in Fig. 7. In Fig. 7(a) and 7(b) we show spectra obtained near the end of the exponential growth phase, comparing a case where the undulator field is large and optical guiding is occurring (this is the example of ref. 10) with a case where the undulator field is weaker and optical guiding is marginal according to the theory and not found experimentally. Because the sideband shift depends on the synchrotron period, which itself depends on the product $(a_{saw})^{1/2}$, we have allowed the

signal in case (b) to grow to larger amplitude than case (a) so that we are comparing examples with nearly the same synchrotron period. This is done by reducing the length of the electron beam in the undulator for the case with larger pump field. An experimental estimate of the synchrotron period is in the range $\sim 20\text{cm}$ (this is obtained from a study of power variation along the electron beam following the point of saturation). The sideband shift from the carrier in Fig. 7(b) is seen to be consistent with this measurement ; that is, $N_{\text{syn}}/N \sim 10\%$.

By comparing the two examples in Figs. 7(a) and 7(b), we find the optical guiding has resulted in an increase of the sideband displacement from the FEL carrier. We attribute this increase to the refractive effect of optical guiding upon the wave group velocity, as given by equation (8). The experiment operates under conditions of refractive guiding dominating gain guiding, which is realized when the gain length is larger than the Rayleigh (diffraction) length. In Fig. 7(c), we show what happens to the spectrum of Fig. 7(a) if the signal is allowed to grow well into the saturation regime. Then the sidebands have a tendency to shift closer to the carrier : the short wavelength sideband returns to the same location as Fig. 7(b), while the long wavelength sideband is shifted somewhere between the location of Fig. 7(a) and Fig 7(b). Again, the synchrotron period is nearly unchanged. The conclusion from Fig. 7(c) is that as the signal goes into saturation, the additional sideband shift due to guiding is diminished. The results are in qualitative agreement with the numerical results discussed earlier.

We are grateful to Prof. S. Johnston for sharing his unpublished results with us. This research is supported by the U. S. Office of Naval Research, Grant No. N0014-79C-0769, and the National Science Foundation, Grant No. ECS-87-13710.

TABLE I

FEL EXPERIMENTAL PARAMETERS

Accelerator Voltage	800Kv (Fig. 5, 6, 7)
	700Kv (Fig. 2, 3)
Electron beam current density	1kA/cm ²
Electron beam radius	2mm
Waveguide (drift tube) radius	9mm (Fig. 5, 6, 7)
	3mm (Fig. 2, 3)
Undulator period	1.7cm (Fig. 5, 6, 7)
	1.45 cm (Fig. 2, 3)
<i>Effective</i> \wedge Normalized vector potential of undulator field \wedge	$(\gamma V_L/c)$ $a_w \sim 0.3$
FEL carrier wavelength	1.8 - 2.0mm (Fig. 5,6, 7)
	2.5mm (Fig. 2, 3)
FEL power	100Kw to Mw's
Resonator length	$\approx 1m$

References

1. N. M. Kroll and M.N. Rosenbluth, in Physics and Quantum Electronics (Addison-Wesley, Reading, MA, 1980), Vol. 7, p.147
2. N.M. Kroll, P.L. Morton, and M.N. Rosenbluth, in Ref. 1, p.81
3. R. W. Warren, B.E. Newnam, and J.C. Goldstein, IEEE J. Quant. Electron. 21, 882 (1985)
4. F.G. Yee, J. Masud, T.C. Marshall, and S.P. Schlesinger, Nucl. Instr. Meth. Phys. Res. A 259, 104 (1987)
5. J. Masud, T.C. Marshall, S.P. Schlesinger, F.G. Yee, W. M. Fawley, E.T. Scharlemann, S.S. Yu, A.M. Sessler, and E. J. Sternbach, Phys. Rev. Lett. 58, 763 (1987)
6. F.G. Yee, T.C. Marshall, and S. P. Schlesinger, IEEE Trans. Plasma Sci. 16, 162 (1988)
7. F. Hartemann, K.Xu, G. Bekefi, J.S. Wurtele, and J. Fajans, Phys. Rev. Lett. 59, 1177 (1987)
8. R. W. Warren and B.D. McVey, Nucl. Instrum. Methods Phys. Res. A 259, 154 (1987)

9. J. E. LeSala, D.A. G. Deacon, and J.M.J. Madey, Phys. Rev. Lett. 59, 2047 (1987)
10. A. Bhattacharjee, S.Y. Cai, S. P. Chang, J.W. Dodd, and T. C. Marshall, Phys. Rev. Lett. 60, 1254 (1988)
11. F.G. Yee and T. C. Marshall, IEEE Trans. Plasma Sci. 13, 480 (1985)
12. B. Hafizi, A. Ting, P. Sprangle and C. M. Tang , Phys. Rev. A 38, 197 (1988)
13. M. N. Rosenbluth, H. V. Wong and B. N. Moore, private communication
14. W. B. Colson, Proc. SPIE 453 , 290 (1984)
15. S. Johnston, A. M. Sessler, Y. -J. Chen, W. M. Fawley, and E. T. Scharlemann, private communication

Figure Captions

- Figure 1 The FEL oscillator. The electron beam length is varied by moving the iron-field deflector. The quartz mirror is an etalon.
- Figure 2 Spectrum showing carrier (2.5mm) and long-wavelength sideband (2.6mm) emitted from an FEL in an untapered undulator (a) and a tapered undulator (b). The sideband amplitude in (b) is smaller by 50% compared with (a) (F. G. Yee, T. C. Marshall and S. P. Schlesinger, IEEE Trans. Plasma Sci. 16, 162 (1988)).
- Figure 3 Power growth along the tapered portion of the undulator.
- Figure 4 Domain of integration in x and y for equations (5) – (7) indicated by the cross-hatched region.
- Figure 5 Numerical simulation of sidebands with (solid lines) and without optical guiding (dotted lines).
- Figure 6 FEL spectra for an oscillator configuration using a single-mesh mirror reflector (b) and a two-mesh etalon (a). The long-wavelength sideband is at 2.25mm.
- Figure 7 Effect of optical guiding on the sideband wavelength. (a) Case of good optical guiding, [10]; (b) optical guiding poor, reduced B_{\perp} ; (c) same as case (a) but the signal is run into saturation.

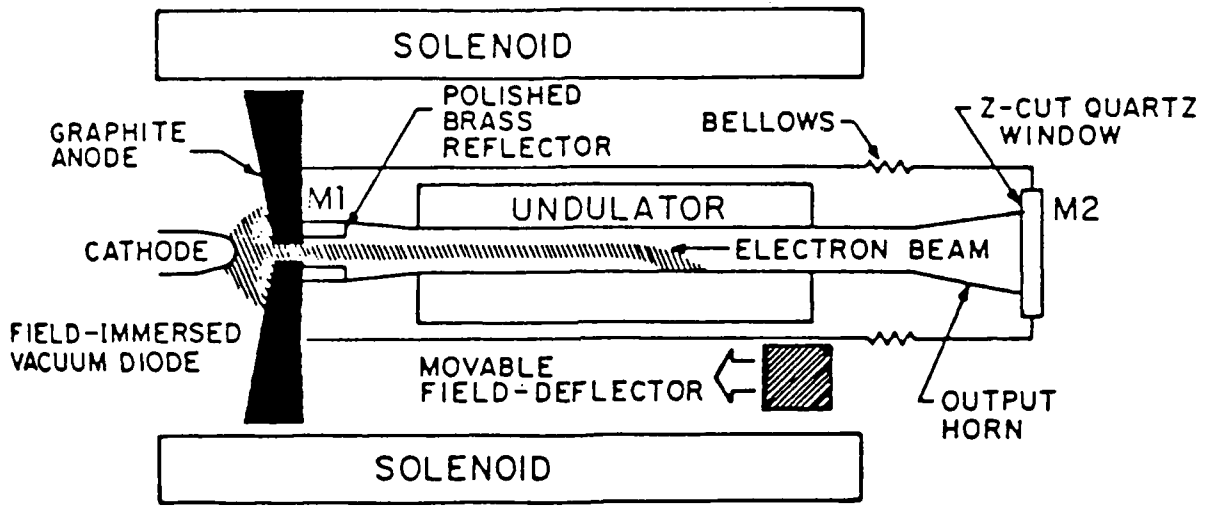
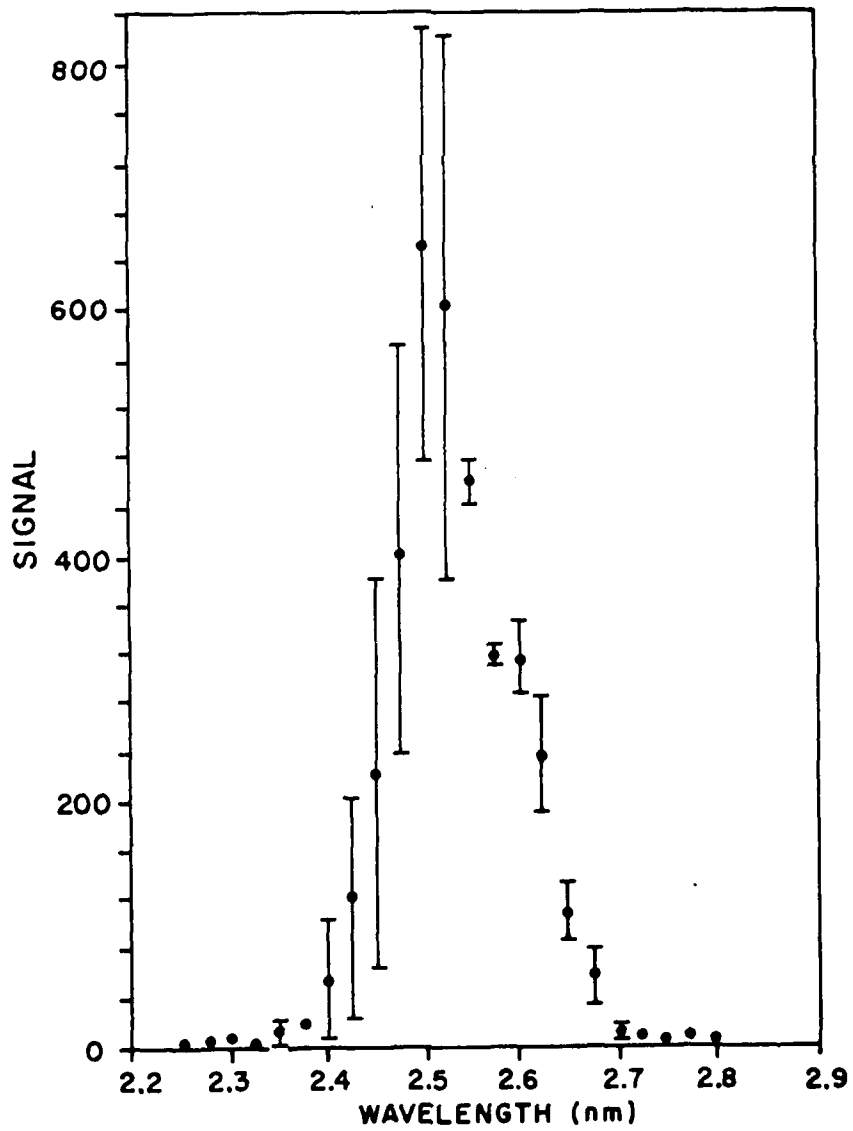
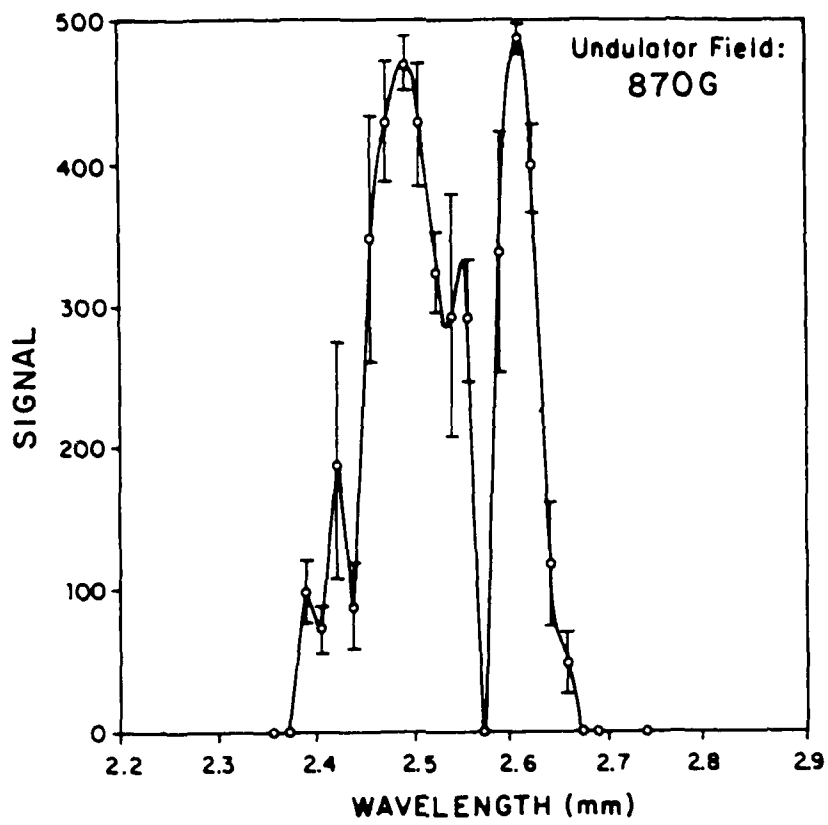


Figure 1



A-PP-1157

(a)

(b)

D

A-PP-1154

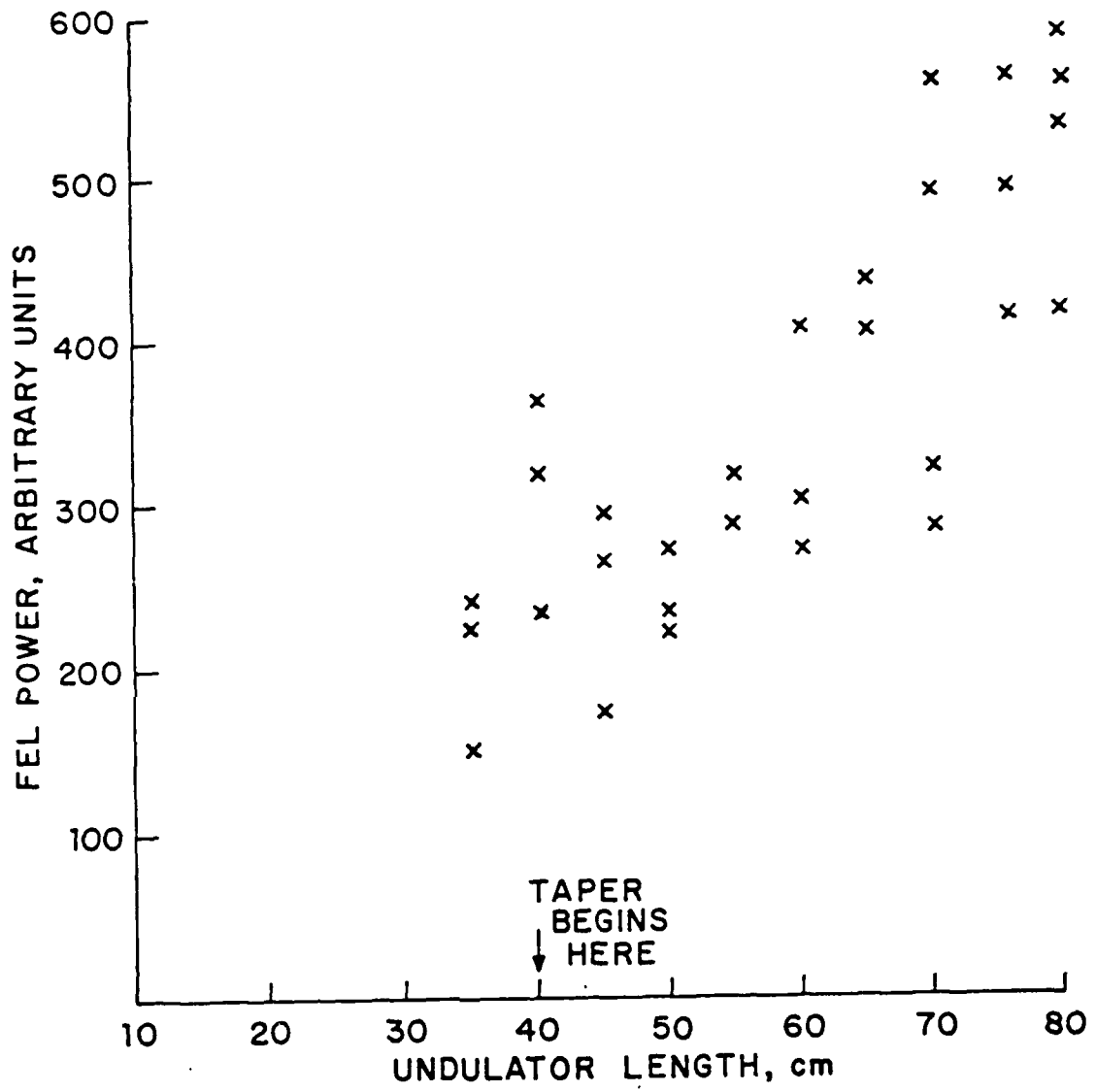


Figure 3

A.P.P.-1155

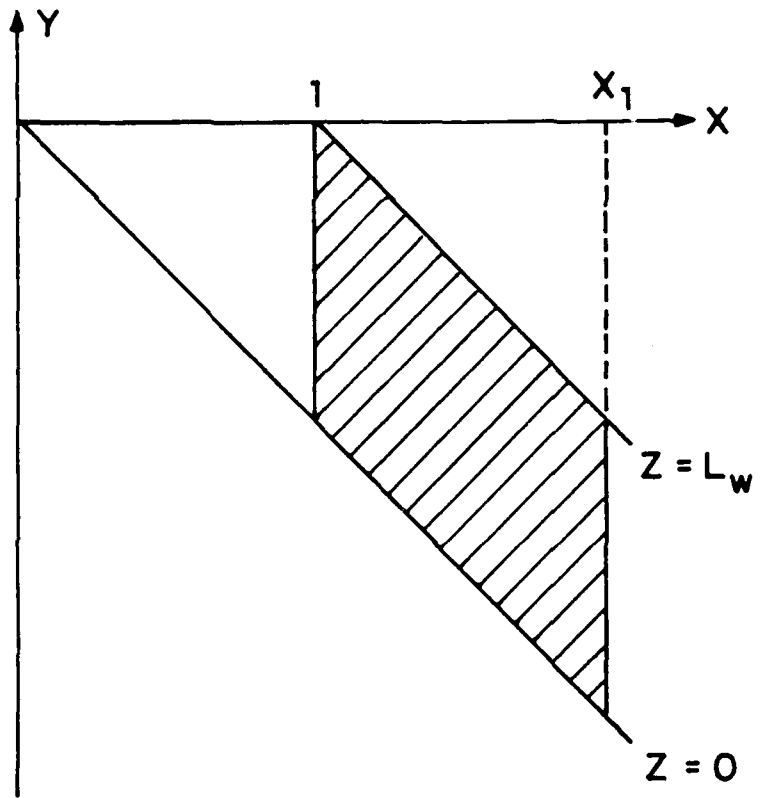


Figure 4

A-PP-1152 . JD

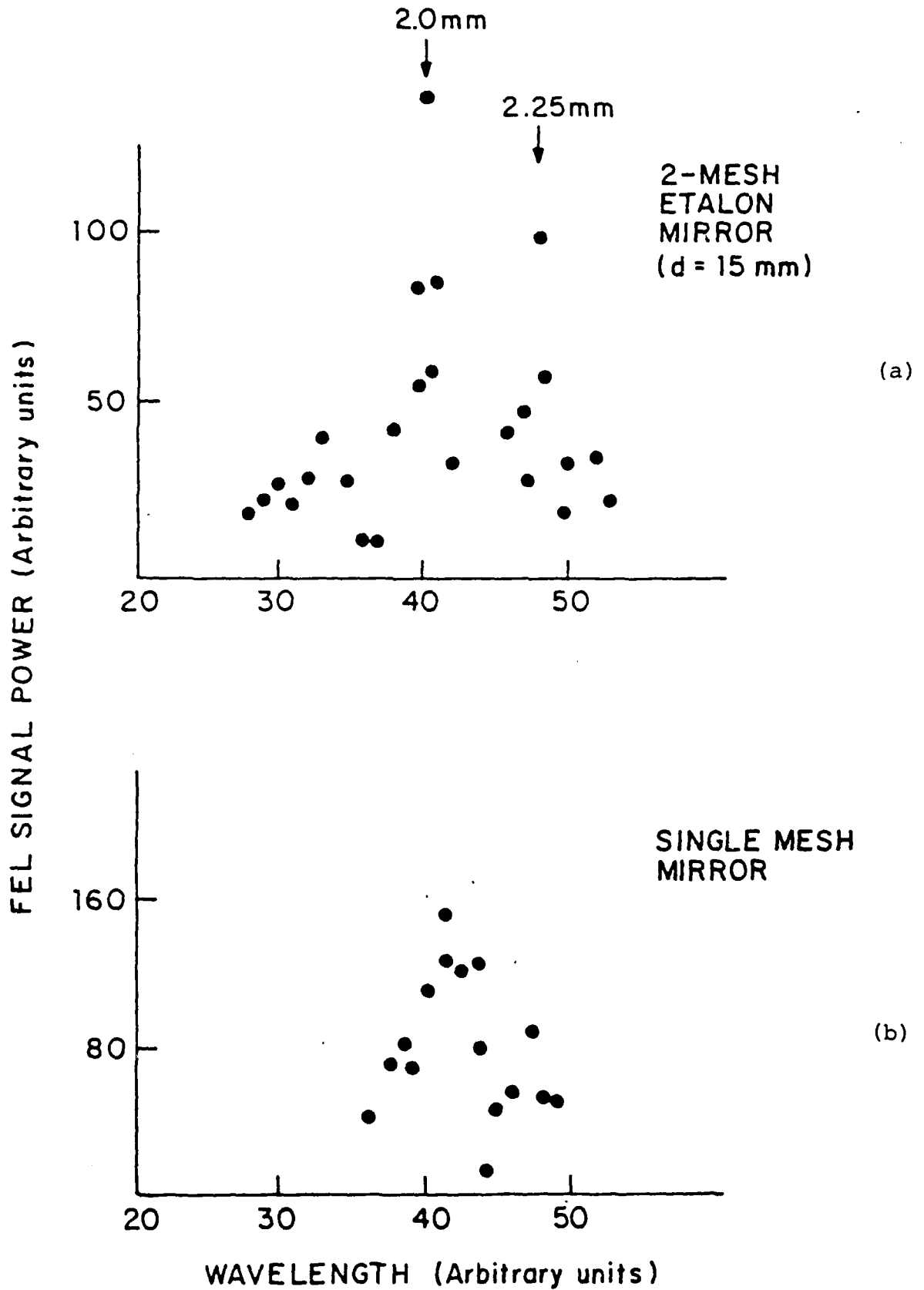


Figure 6

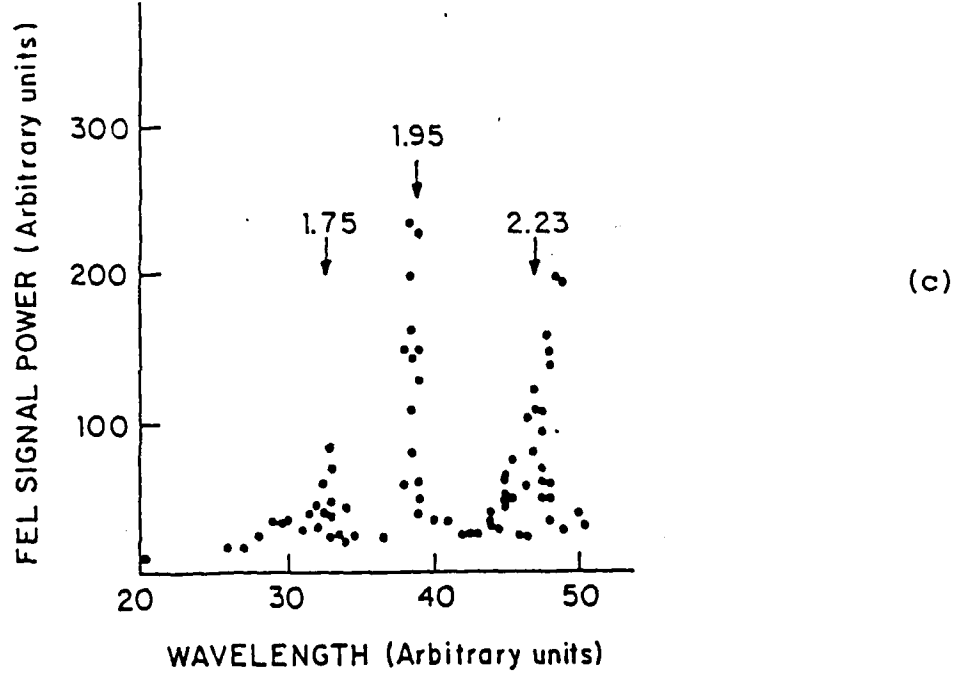
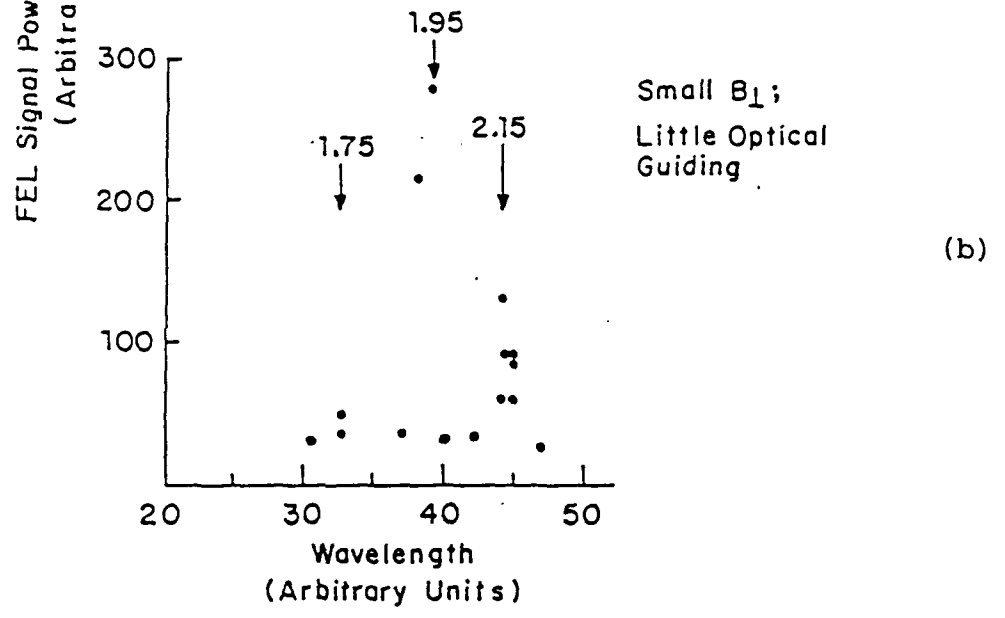
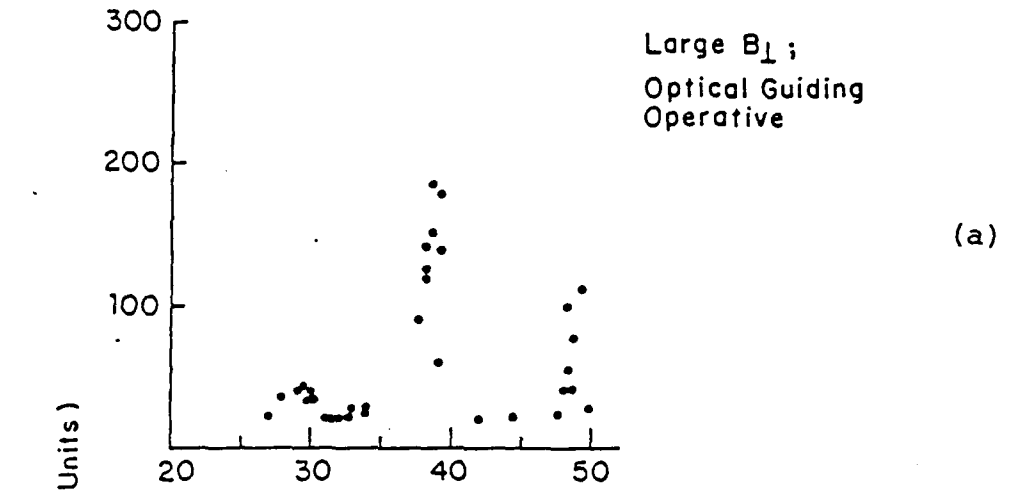


Figure 7